Deep-Sea Research II 55 (2008) 1389–1397

Contents lists available at ScienceDirect

Deep-Sea Research II

journal homepage: www.elsevier.com/locate/dsr2

# The distributions of, and relationship between, $^3$He and nitrate in eddies

W.J. Jenkins *, D.J. McGillicuddy Jr., D.E. Lott III

*Department of Marine Chemistry and Geochemistry, Woods Hole Oceanographic Institution, Woods Hole, MA 02543, USA*

ARTICLE INFO

*Article history:*
Accepted 4 February 2008
Available online 9 May 2008

*Keywords:*
Biogeochemical tracers
Tracer techniques
$^3$He
Eddies
Atlantic Ocean
Sargasso Sea

ABSTRACT

We present and discuss the distribution of $^3$He and its relationship to nutrients in two eddies (cyclone C1 and anticyclone A4) with a view towards examining eddy-related mechanisms whereby nutrients are transported from the upper 200–300 m into the euphotic zone of the Sargasso Sea. The different behavior of these tracers in the euphotic zone results in changes in their distributions and relationships that may provide important clues as to the nature of physical and biological processes involved.

The cyclonic eddy (C1) is characterized by substantial $^3$He excesses within the euphotic zone. The distribution of this excess $^3$He is strongly suggestive of both past and recent ongoing deep-water injection into the euphotic zone. Crude mass balance calculations suggest that an average of approximately $1.4 \pm 0.7$ mol m$^{-2}$ of nitrate has been introduced into the euphotic zone of eddy C1, consistent with the integrated apparent oxygen utilization anomaly in the aphotic zone below. The $^3$He–$NO_3$ relationship within the eddy deviates substantially from the linear thermocline trend, suggestive of incomplete drawdown of nutrients and/or substantial mixing between euphotic and aphotic zone waters.

Anticyclone (A4) displays a simpler $^3$He–$NO_3$ relationship, but is relatively impoverished in euphotic zone excess $^3$He. We suggest that because of the relatively strong upwelling and lateral divergence of water the residence time of upwelled $^3$He is relatively short within the euphotic zone of this eddy. An estimate of the recently upwelled nutrient inventory, based on the excess $^3$He observed in A4's lower euphotic zone, is stoichiometrically consistent with the oxygen maximum observed in the euphotic zone.



## 1. Introduction

Tracer-based estimates of net community production (Jenkins and Goldman, 1985; Musgrave et al., 1988; Spitzer and Jenkins, 1989), export production (Jenkins, 1984, 1998; Jenkins and Wallace, 1992), and new production (Jenkins, 1988a; Jenkins and Doney, 2003) in the Sargasso Sea point to rates of nutrient supply to the euphotic zone in this area that are difficult to reconcile with traditional concepts for material transport within the oligotrophic subtropical gyre (e.g., Lewis et al., 1986; Oschlies, 2001; Williams and Follows, 1998). Based on calculations of nutrient flux divergence in the Gulf Stream (Pelegri and Csanady, 1991; Pelegri et al., 1996), Jenkins and Doney (2003) proposed the subtropical nutrient spiral as a mechanism to supply thermocline nutrients to the seasonal layer of the subtropical gyre. It has been hypothesized that nutrient transport to the euphotic zone is subsequently achieved by winter-time convection, turbulent mixing, or vertical transport by eddies (McGillicuddy et al., 1998, 2003; McGillicuddy and Robinson, 1997; Williams et al., 2006). Regarding this last mechanism, a high-resolution model simulation (McGillicuddy et al., 2003) appears to achieve the nutrient fluxes implied by $^3$He flux-gauge calculations for new production, and tritium–$^3$He-based estimates of export production in the subtropical North Atlantic, but another (Oschlies, 2002) suggests that this mechanism falls short of the target flux by an order of magnitude.

The root of this conundrum lies in the fact that the tracer-based techniques point to apparent vertical nutrient fluxes as much as an order of magnitude greater than the traditional paradigm for oligotrophic waters (e.g., Eppley and Peterson, 1979). Estimates of aphotic zone oxygen utilization rates near Bermuda (Jenkins, 1977, 1980, 1998; Jenkins and Doney, 2003) provide us with a long-term estimate of export production that is consistent with a new production rate that requires a nutrient supply approaching 0.8 mol N m$^{-2}$ yr$^{-1}$. One potential caveat associated with this estimate is that the aphotic zone oxygen utilization rate estimate is by nature an integrated measure, so it may reflect a more regional or large-scale average. On the other hand, new production estimated from mixed-layer $^3$He excesses (Jenkins, 1988a, b; Jenkins and Doney, 2003) yield very similar results, but are intrinsically a *local* measure of new production, albeit on seasonal to annual time scales. In essence, $^3$He is produced within the aphotic zone by *in situ* decay of tritium, very much like the

* Corresponding author. Tel.: +1 508 289 2554.
*E-mail address:* wjenkins@whoi.edu (W.J. Jenkins).

0967-0645/$ - see front matter © 2008 Elsevier Ltd. All rights reserved.
doi:10.1016/j.dsr2.2008.02.006

ingrowth of inorganic nutrients by the remineralization of falling organic matter. That is, one may regard $^3$He as a pseudo-nutrient whose reflux to the euphotic zone is unambiguously physical in nature. The fact that the estimated $^3$He flux is quantitatively consistent with the long-term budgets and evolution of this isotope in the main thermocline (Jenkins, 1998; Jenkins and Doney, 2003) supports the calculation. One complication, however, is that within the euphotic zone $^3$He and nutrients become decoupled. This does not invalidate the underlying assumptions of the flux gauge calculation, but it makes interpretation of the detailed distributions more challenging. Based on the premise that one scientist's noise is another's signal, however, we would argue that changes in the relationship between $^3$He and the more labile nutrients is an important diagnostic that may provide information about underlying processes.

The EDDIES Program presented us with an opportunity to directly observe in detail the distributions of $^3$He and nutrients within well-characterized and "representative" eddies (both cyclones and anticyclones) in the Sargasso Sea. Our starting premise was that the distribution of $^3$He may provide a rough constraint on the magnitude of upward transport of nutrients, that its relatively longer persistence in the euphotic zone (below the mixed layer) may allow us to set limits on how much nutrient has been utilized since arrival within the euphotic zone, and that the detailed relationships between $^3$He and nutrients may be diagnostic of the nature of upward transport, uptake and remineralization within these features.

## 2. Methods

Tritium and $^3$He sampling for the EDDIES program was done as part of four survey cruises aboard the R/V *Oceanus* in the northwestern Sargasso Sea, two each in the summers of 2004 (OC404-1 and OC404-3) and 2005 (OC415-1 and OC415-3). Water samples were taken using a 24-bottle (10 L) CTD Rosette system from a number of hydrographic casts positioned to characterize mesoscale features (see Fig. 1). Locations relative to eddy center were established by a combination of satellite altimetry and hull-based acoustic velocimetry (see McGillicuddy et al., 2007), and other supporting measurements, including dissolved oxygen, pigments, and nutrients, were performed according to standard JGOFS protocols (see other articles in this issue). Samples for $^3$He were obtained using standard WOCE/CLIVAR sampling procedures. Valved stainless steel sample cylinders were gravity filled from rosette Niskin bottles using Tygon tubing, and helium subsequently extracted on shipboard into aluminosilicate glass ampoules (Lott and Jenkins, 1998) for shore-based mass spectrometric isotopic analysis (Lott and Jenkins, 1984). Tritium samples were drawn into argon-filled, baked glass bottles and degassed on shore in aluminosilicate flasks for measurement by $^3$He regrowth (Clarke et al., 1976). Helium isotope ratios were determined to an accuracy of 0.15%, as determined from reproducibility of analytical standards, and from replicate analyses made on numerous other cruises. The results are expressed in terms of an isotope ratio anomaly relative to the atmospheric standard:

$$\delta^3\mathrm{He} = \left(\frac{(^3\mathrm{He}/^4\mathrm{He}_X)}{(^3\mathrm{He}/^4\mathrm{He}_{\mathrm{AIR}})} - 1\right) \times 100\%$$

Tritium measurements are made using $^3$He regrowth and mass spectrometric peak-height manometry, using an atmospheric standard and assuming an atmospheric helium abundance of 5.24 ppm by volume (Holand and Emerson, 1987; Oliver et al., 1984), atmospheric $^3$He/$^4$He ratio of $1.384 \times 10^{-6}$ (Clarke et al., 1976), and a tritium half-life of 4500 days (Lucas and Unterweger, 2000). Tritium concentrations are expressed in Tritium Units (TU), i.e. the atom ratio of tritium to hydrogen multiplied by $10^{18}$, decay corrected to the date of sampling, and were measured to an accuracy of 0.5% of the value and a detection limit of 0.005 TU, added together in quadrature.

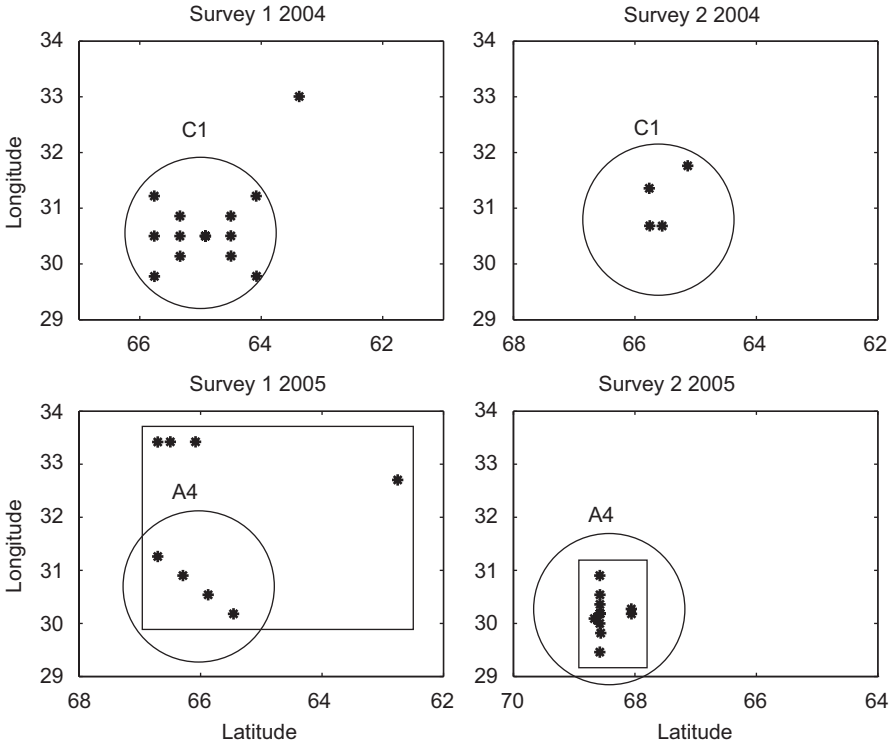


**Fig. 1.** Location of sampling during the EDDIES cruises. The circles indicate the approximate locations of the eddy of interest during each survey.

Helium and tritium sampling was performed at 36 stations occupied during the four survey cruises: two in the summer of 2004 and two in the summer of 2005. Fig. 1 is a plot of stations occupied for $^3$He measurements during the four surveys, and the circles denote the approximate locations, at the time of each cruise, of the eddy of interest (cyclone C1 in 2004 and anticyclone A4 in 2005).

## 3. Results

For the purpose of discussing a "flux-gauge" ratio, we must estimate the current regional thermocline co-relationship between $^3$He and nitrate, which gradually evolves over time since $^3$He is a transient tracer. The rationale is that ultimately the supply of nutrients for new production in this region is advection of thermocline nutrients via the "Nutrient Spiral" into the seasonal layer, where it is subsequently acted on by winter convection, diapycnal mixing, and vertical motions associated with eddies. We obtain the slope of this relationship by regressing $\delta^3$He vs. nitrate for ~200 upper thermocline samples (i.e. for depths shallower than ~700 m, and nitrate+nitrate concentrations $<10\,\mu mol\,kg^{-1}$) obtained from the CLIVAR repeat lines A20 and A22 at 52°W and 65°W occupied in 2003. The slope thus obtained is $2.39\pm0.06\,\mu mol\,kg^{-1}\,\%^{-1}$. This slope is virtually identical with the slope obtained from the 2004 and 2005 Eddies Cruises of $2.38\pm0.17\,\mu mol\,kg^{-1}\,\%^{-1}$ derived from 44 samples taken at depths greater than 200 m. Thus, for purposes of discussion, we hereafter define a "regional nitrate:$^3$He ratio" of $2.4\pm0.1\,\mu mol\,kg^{-1}\,\%^{-1}$. It should be noted that this slope differs from the $0.8\pm0.2\,\mu mol\,kg^{-1}\,\%^{-1}$ obtained and used earlier by Jenkins (1988a, b, 1998) and the $0.97\pm0.06\,\mu mol\,kg^{-1}\,\%^{-1}$ reported by Jenkins and Doney (2003) due to the fact that $^3$He is a transient tracer: the thermocline $NO_3$:$^3$He ratio has been increasing steadily with time.

### 3.1. The distribution of $^3$He in cyclone C1

During the first survey cruise, we attempted to map out the distribution of $^3$He in cyclonic eddy C1. This eddy is characterized by very intense aphotic zone oxygen minimum at 200–400 m depth, containing oxygen concentrations lower than ever observed in this stratum at this locale over the entire history of observations (from Station S post 1960 onward). Notably, the oxygen minimum appeared associated with a corresponding $T$–$S$ anomaly, which may be indicative of a remote origin (McGillicuddy et al., 2007). How this deep oxygen anomaly was created, i.e. whether it has been advected from some low oxygen region or locally formed by remineralization, has implications for our understanding of the biogeochemical processes within and physical transport of these eddies. Unfortunately, none of the $^3$He stations in this first survey intersected the intense oxygen minimum.

Fig. 2 shows contour maps of $\delta^3$He (the helium isotope ratio anomaly with respect to atmosphere) at four depths in cyclonic eddy C1 from the first survey. Major contours (solid lines) are in percent, and the dashed contour interval is 0.25%. Note that measurement precision is 0.15% (one standard deviation) and that seawater in equilibrium with the atmosphere will have a $\delta^3$He = −1.66% (Benson and Krause, 1980); that is, $^3$He is slightly

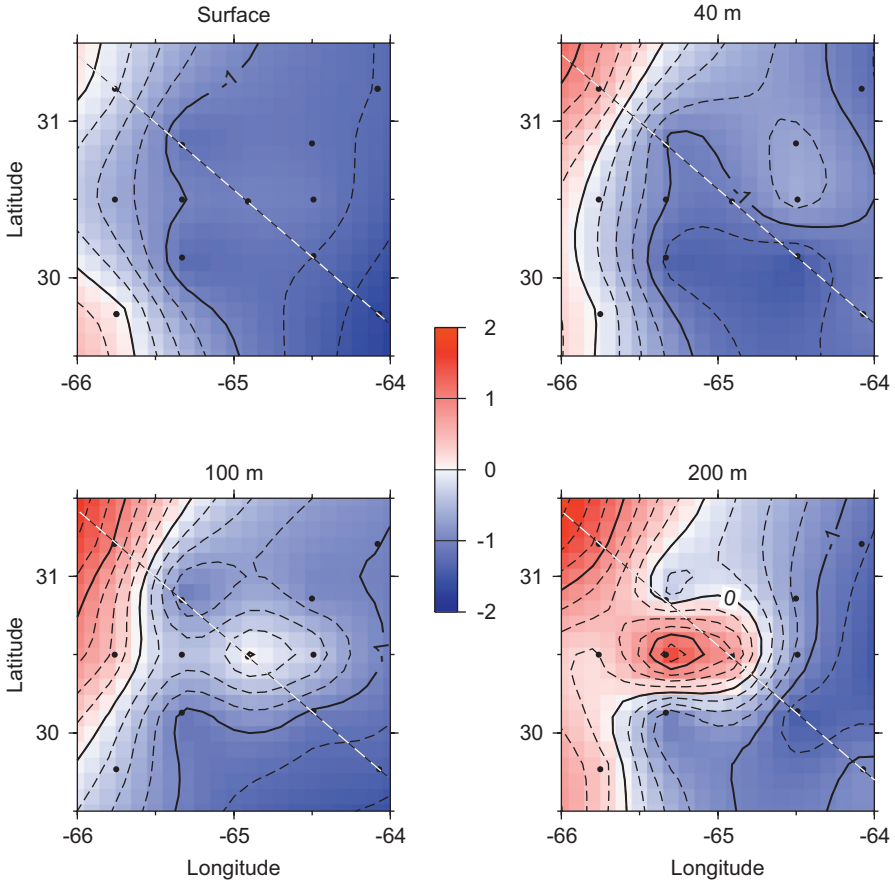


**Fig. 2.** Contours of helium isotope ratio anomaly $\delta^3$He (in %) at selected depths for cyclonic eddy C1. The dashed white diagonal line corresponds to the section shown in Fig. 3. The dashed contour interval is 0.25%, slightly less than 2 standard deviations of measurement.

less soluble than $^4$He. There is clear evidence of enhanced subsurface $^3$He excess both in the core of C1 and along the western/northwestern rim of the eddy. It is striking that the excess $^3$He in the western rim of the eddy extends to the surface, despite the expectation that gas exchange would tend to remove this excess. At first glance, one might argue that this appears to be part of a regional pattern that is evident in the WOCE and CLIVAR Repeat Hydrography sections A20 and A22, which show an outcropping of $\delta^3$He isopleths in the general vicinity of the Gulf Stream much farther north, but the anomalies observed here are approximately 500 km farther south.

The surface water excess in $^3$He relative to the expected solubility isotope ratio anomaly ($\delta^3He_{Sol} = -1.66\%$) to the west of the eddy core exceeds 1.5%, or about 10 standard deviations of measurement uncertainty, and is therefore quite significant. The presence of this excess in surface waters suggests ongoing upwelling of this tracer, or mixing from $^3$He-rich waters below in recent history, since gas exchange would erase this anomaly within only a week or two. It is conceivable that this excess is a relict of late winter convection, where significant amounts of $^3$He may have been trapped beneath rapidly stratified waters in spring, and subsequently "mined" into the mixed layer by eddy or frontal motions after stratification. On deeper horizons, the northwest–southeast gradient gradually merges into a distinct maximum located near the eddy core. There is a vague impression of cyclonic twisting of isopleths around the core (note the bending of isopleths north of the eddy core toward the west on the 100 and 200 m levels). The apparent connection between the eddy core and the western limb of the eddy appears more pronounced at 200 m than 100 m, but the station spacing is not adequate to truly resolve this. Moreover, because the survey occurred over the course of a few days, the picture is not perfectly synoptic so caution must be exercised in interpreting spatial structure.

Fig. 3 shows a section taken diagonally through eddy C1 in a southeast–northwest transect (see dashed white line in Fig. 2). Property contours are white, while contours of potential density anomaly (in kg m$^{-3}$) are superimposed in black. This section shows the rising isopleths for both $^3$He (upper panel) and nitrate (middle panel) in the center of the eddy, but also an upward slope in $\delta^3$He isopleths toward the northwest in the deeper water. Compared to $^3$He, nitrate appears to more faithfully follow isopycnal surfaces. This is anticipated because both radiative

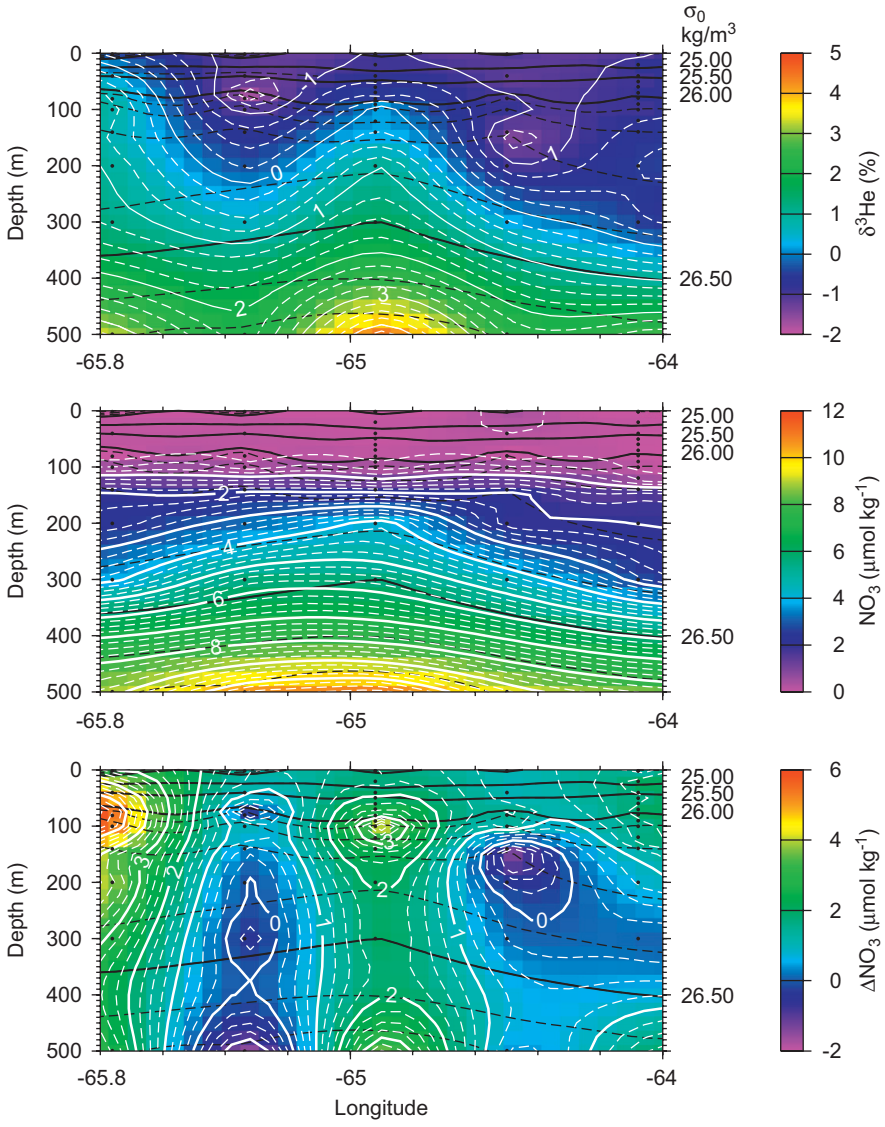


**Fig. 3.** A southeast–northwest depth section (see diagonal dashed white line in Fig. 2 for location) through cyclone C1 for $\delta^3$He (in % upper panel), nitrate (in μmol kg$^{-1}$ middle panel), and $\Delta NO_3$ (missing nitrate in μmol kg$^{-1}$ lower panel). Property contours are white, while the superimposed black contours are potential density anomaly in kg m$^{-3}$.

heating and photosynthetic nutrient utilization are coupled strongly to the light field, which penetrates to nearly 100 m depth, while $^3$He is only lost by gas exchange processes in the surface mixed layer. The presence of significant $^3$He excesses in the upper 100 m, where nutrient levels are typically very low, and the tendency for $\delta^3$He isopleths to cross isopycnals, implies the existence of upwelled nutrients in the recent past. We estimate the inventory of excess $^3$He in the upper 100 m to be $\sim 130 \pm 30\%$ m averaged over the entire eddy. This calculation is a lower bound, since there likely has been significant loss of $^3$He due to gas exchange with the atmosphere. That is, it is based on the standing stock of this isotope within the euphotic zone, and the actual fluxes may be significantly higher. Using the regional $NO_3$:$^3$He ratio, this implies a lower bound nutrient loading (and subsequent removal) of $0.3 \pm 0.1$ mol $(NO_3)$ m$^{-2}$. This represents an average over the entire eddy, and is higher both over the eddy core and on the western and northwestern rim.

We stress again that this estimate represents a lower bound, since $^3$He is being continuously lost from the ocean by gas exchange to the atmosphere. This loss rate can be estimated based on the mixed-layer $^3$He excesses. An area-average mean-mixed-layer $\delta^3$He is $-1.1\%$, being significantly larger in the west and somewhat lower in the east. We estimate an average gas exchange piston velocity for $^3$He of 7 m d$^{-1}$ based on a standard gas-exchange formulation (Wanninkhof, 1992) and using NCEP reanalysis winds for the 2 weeks bracketing station occupation. This corresponds to a $^3$He efflux of order $8 \pm 2\%$ m d$^{-1}$. The significance of this flux is that it would easily exhaust the mixed-layer $^3$He inventory within about a week, and were it not for stratification below the mixed layer the euphotic zone inventory would be removed in less than 3 weeks. Thus, the presence of significant excess $^3$He in the mixed layer points to a dynamically maintained balance of this isotope within the mixed layer and more importantly in the euphotic zone. If the flux we estimate were maintained over the period of time since seasonal stratification occurred (a period of 60–90 days), and the existing standing stock of $^3$He were maintained (a likely conservative assumption), the integrated flux of $^3$He to the atmosphere and by inference into the euphotic zone would be about $600 \pm 300\%$ m, which would yield a nitrate flux of approximately $1.4 \pm 0.7$ mol m$^{-2}$. Such an estimate may be considered conservative for three reasons. First, it is tied to the assumption that the time period in question is bounded between the recent intensification of the eddy (May 2004) and may in fact extend over the longer lifetime of the eddy, which can be traced back with satellite altimetry to February 2004 (McGillicuddy et al., 2007). Second, it is likely that past surface layer concentrations of excess $^3$He would have been higher after winter convection. Third, wind speeds, and hence gas exchange rates, are typically higher earlier in the year. The implied nutrient flux is broadly similar in magnitude to the estimate of $0.7 \pm 0.2$ mol N m$^{-2}$ for export production obtained by integrating the aphotic zone apparent oxygen anomaly relative to waters just outside of the eddy (McGillicuddy et al., 2007). The ephemeral nature of the deeper feature, that is the observed erasure of the aphotic zone oxygen minimum between June and August, suggests that the productivity event either occurred relatively recently prior to our first survey cruise or that it was even more intense or pervasive at some earlier time. $^{234}$Th measurements show no evidence of enhanced POC fluxes within the past 2 months (Buesseler et al., 2007).

In principle, something can be learned from the spatial structure of the relationship between $^3$He and nitrate. As fluid parcels are upwelled or mixed into the base of the euphotic zone, but below the mixed layer, nitrate will be removed by photosynthesis, leaving $^3$He behind. If the ultimate source of new nutrients into the euphotic zone is physical transport (advection and mixing) of waters from the main thermocline, then we can use the regional $^3$He:$NO_3$ relationship to derive a new quantity, "missing nitrate", as the difference between the nitrate level would be predicted from the observed excess $^3$He concentration and the observed nitrate concentration using

$$\Delta NO_3 = 2.4 \times (\delta^3\mathrm{He} + 1.66) - NO_3$$

A positive value in $\Delta NO_3$ should correspond to the amount of nitrate that has been removed, and a negative value should indicate the presence of recently remineralized nutrients. Uncertainty in this derived quantity, associated with analytical errors in the isotope ratio anomaly and nutrient measurements, should be approximately 0.4–0.5 μmol kg$^{-1}$.

The bottom panel in Fig. 3 is a plot of $\Delta NO_3$ in the upper 500 m corresponding to the $^3$He and nitrate sections in the panels above. The largest positive value of $\Delta NO_3$ was observed in the northwest end of the section, at the base of the euphotic zone, and below the mixed layer. This is consistent with the scenario described above, with a significant inventory of $^3$He (and by inference nitrate) being trapped below the mixed layer on spring stratification, and subsequent removal of nutrients, producing positive $\Delta NO_3$. The presence of significant excess $^3$He in the mixed layer above, however, suggests that there is, or recently has been, a net upward flux of this isotope into the mixed layer.

The eddy itself is characterized by a more modest bolus of high $\Delta NO_3$ concentrated at the base of the euphotic zone in its core, but is surrounded by lower $\Delta NO_3$. This structure of low $\Delta NO_3$ is hinted at by the apparent horseshoe-shaped feature in the level maps of $^3$He shown in Fig. 2. The presence of some modestly negative values of $\Delta NO_3$ is suggestive of local remineralization, but we note that these particular features are barely resolved given the uncertainty of 0.4–0.5 μmol kg$^{-1}$ in this derived quantity. It is tempting to interpret the pattern as suggestive of upward transport of thermocline nutrients in the center of eddy, but with export and remineralization being most pronounced away from eddy center. However, this would be inconsistent with observations of the intense aphotic zone oxygen minimum at eddy center reported by McGillicuddy et al. (2007). It should be noted that the observed oxygen minimum feature was extremely compact, and unfortunately not caught by the $^3$He sampling grid, which occurred prior to the discovery of the feature.

In conclusion, cyclone C1 shows evidence of recent, active supply of $^3$He (and by inference nutrients) into the euphotic zone. The area-averaged amounts of nutrient injection span a range from a minimum of 0.3 mol m$^{-2}$, based on observed euphotic zone inventories of excess $^3$He, to approximately 1.4 mol m$^{-2}$ or more, depending on assumptions about past behavior. There appears to be a locus of injection associated with the core of the eddy, with subsequent streamers of material spiraling outward between the mixed layer and the base of the euphotic zone. However, there are clear regional gradients that the eddy appears to be working on, suggesting that some of the computed flux may be a relict of winter convection. Finally, the distribution of the deviations from the regional $^3$He–$NO_3$ relationship, e.g. the missing nitrate, shows evidence of a spring bloom event in the northwest, eddy-driven upwelling in the center, and a hint of eddy-related remineralization just outside the eddy core.

### 3.2. The distribution of $^3$He in anticyclone A4

Fig. 4 shows north–south sections in the upper 200 m of $\delta^3$He, nitrate and dissolved oxygen across anticyclone A4, sampled in the summer of 2005. Here again there is evidence of excess $^3$He within the euphotic zone, where there is little nitrate. The greater $^3$He excesses occur near the eddy core, and appear associated with

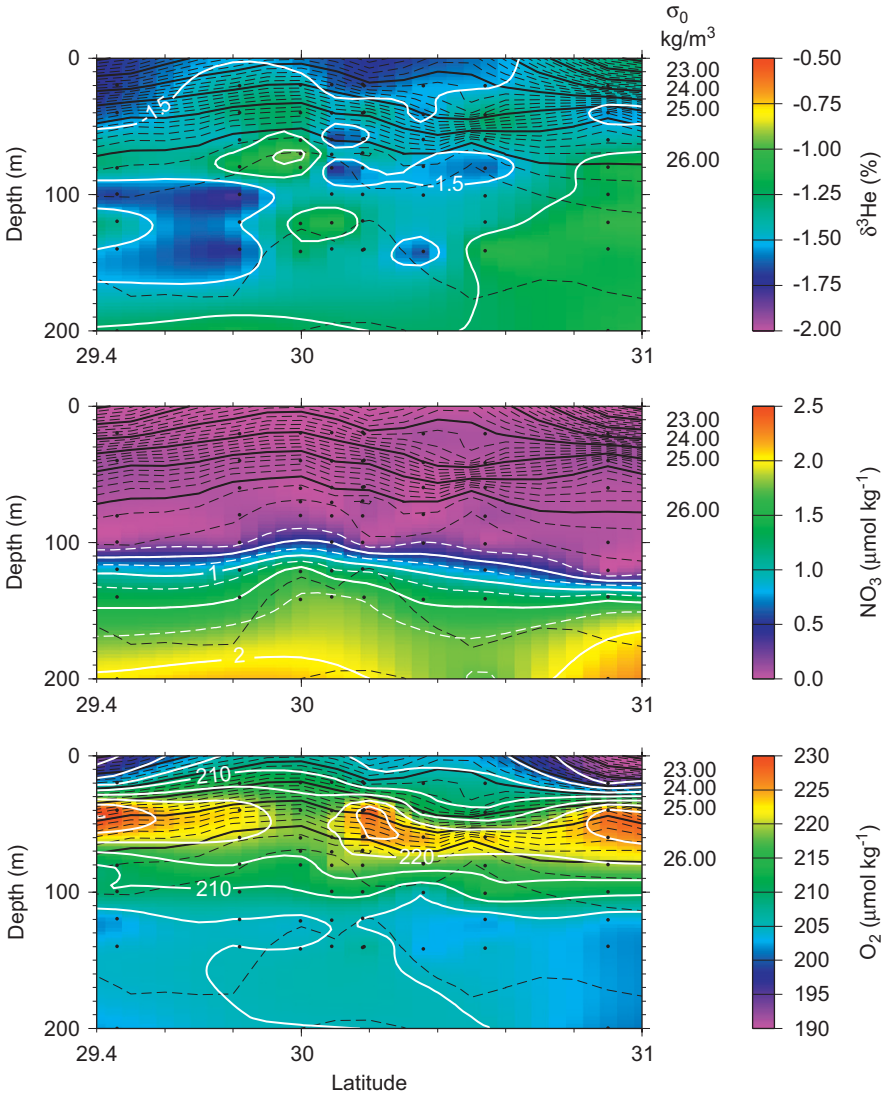


**Fig. 4.** A north–south depth section through anticyclone A4 for $\delta^3$He (in % upper panel), nitrate (in μmol kg$^{-1}$ middle panel), and dissolved oxygen (in μmol kg$^{-1}$ lower panel). Property contours are white, while the superimposed black contours are potential density anomaly in kg m$^{-3}$.

the maximum vertical deflection below in the nitrate isopleths. However, there is also a substantial amount of sub-mesoscale variability: note the juxtaposition of lower values next to higher values near 80 m depth. There is also a trend of increasing $^3$He excess at the northern periphery of the eddy.

Compared to eddy C1, the surface waters are closer to solubility equilibrium in $\delta^3$He, suggesting a very small flux to the atmosphere, if any. Within the euphotic zone, the average $\delta^3\text{He} = -1.45 \pm 0.04\%$, leading to an average excess $^3$He inventory of $21 \pm 5\%$ m, which in turn represents a standing stock of missing nitrate of only $0.05 \pm 0.02$ mol N m$^{-2}$. The contrast with eddy C1 is striking. Despite the expectation of active upwelling due to interaction between an anticyclone and the wind field (see Martin and Richards, 2001, and Ledwell et al., 2008), there is only modest evidence of this in the $^3$He distribution. The explanation may be that much of the $^3$He and nutrients that have been upwelled over the course of this eddy's lifetime have been swept away by divergent flow associated with the upwelling. That is, the observed standing stock represents but a fraction of the eddy's upwelling history. Indeed, the outcropping of dissolved oxygen isopleths at the eddy center and the apparently annular distribution of oxygen supersaturation at about 50–60 m depth, a sign of net community production (Jenkins and Goldman, 1985; Spitzer and Jenkins, 1989), are suggestive of upwelling at eddy center driven by divergent lateral flow. The average excess $\delta^3$He within the lower euphotic zone of the core of A4 is approximately 0.6% over the solubility equilibrium value. Applying the regional $^3$He:$NO_3$ ratio, this implies a missing nitrate on the order of 1.5 μmol kg$^{-1}$. Assuming that carbon fixation will occur in close to Redfield ratios (Anderson and Sarmiento, 1994) the corresponding oxygen produced would be ~20 μmol $O_2$ kg$^{-1}$. Aphotic zone water with this nitrate concentration occurs at about 150 m in the core of this eddy, and has an oxygen concentration of about 205 μmol $O_2$ kg$^{-1}$. A 20 μmol $O_2$ kg$^{-1}$ enhancement of oxygen triggered by eddy-induced upwelling would thus yield concentrations of 220–225 μmol $O_2$ kg$^{-1}$, roughly comparable to that observed in the shallow oxygen maximum of A4.

## 4. Discussion

### 4.1. On the relationship between $^3$He and nitrate in eddies

On the very largest scales, i.e. away from biological sources or sinks, one would expect the distribution of $^3$He and nutrients to be governed by the physical processes of mixing and advection. This

is supported by the roughly linear relationship between the two tracers throughout the upper thermocline of the subtropical North Atlantic. That is, a plot of $\delta^3$He vs. $NO_3$ for thermocline waters within the North Atlantic subtropical gyre (i.e. east of the Gulf Stream, north of the subtropical front, and south of the Azores Front) can be characterized by a linear relationship with a slope that varies by no more than 10–15% at any one time. One can rationalize this linear relationship as arising within the thermocline from the parallel processes of "aging" of the tritium–$^3$He clock and continued buildup of nutrients by remineralization. Differences in slope may arise from regional differences in the integrated balance between ventilation and remineralization rates, but broadly speaking the approximately constant relationship suggests either that the contrasts within the subtropical gyre are not overwhelmingly large, or that the competing processes tend to regionally co-vary.

As fluid parcels move toward the surface layers, however, these tracers become decoupled. Fig. 5 is a schematic of how the linear relationship might break down. As fluid mixes up the regional flux line into the euphotic zone, nitrate is removed by biological uptake. Since this first occurs below the mixed layer, no $^3$He is lost, so the trajectory is directly downward in the diagram toward the lower ellipse marked "uptake". Fixed organic material will be exported from the euphotic zone and remineralized at depths below. Here again, since $^3$He is not transported in this process, the trajectory is vertical toward the upper ellipse marked "remineralization".

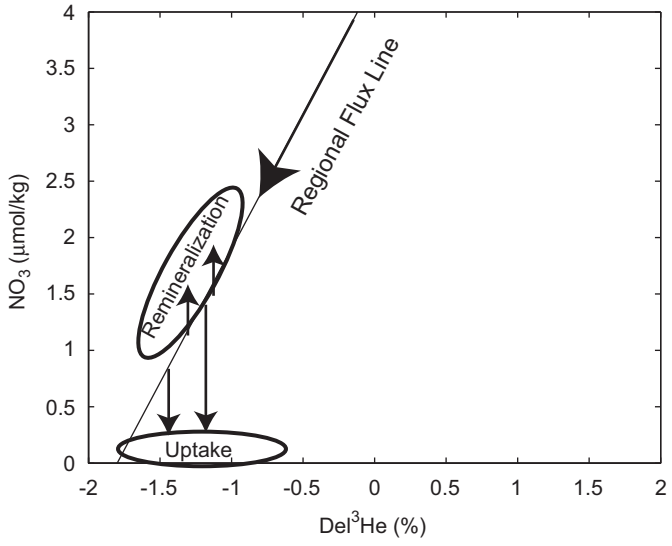


**Fig. 5.** A schematic of the effects of biological uptake and remineralization on the $^3$He–$NO_3$ relationship.

This is essentially what is observed for the $^3$He–$NO_3$ relationship for anticyclone A4 (Fig. 6A). In some respects, this should be expected, since vertical motions (upwelling in the core of the eddy) are well defined and follow the conceptual model described above. Departures from the regional flux line include (1) a set of points along the abscissa reflecting uptake of upwelled nitrate, and (2) a set of points with nitrate in excess of that predicted by the regional flux line. This latter aspect may be a result of differences in the $^3$He–$NO_3$ relationship caused by relatively recent ventilation of the mode waters that comprise the core of the eddy. That is, deep convection in the winter months may result in removal of $^3$He by gas exchange, while nutrient removal and biomass production might be light limited due to deep vertical mixing. Alternatively, it could reflect local remineralization of sinking organic matter produced by the eddy-induced bloom. However, during our occupations of the eddy, sediment trap measurements and $^{234}$Th-based flux estimates indicated export fluxes that were not significantly different from the long-term summertime mean at BATS (Buesseler et al., 2008). The apparent contrast between the $^3$He–$NO_3$ and $^{234}$Th findings still may be consistent since the $^{234}$Th-based measurements represent a 2 to 3 month snapshot of the current and recent (compared to the half-life of $^{234}$Th) export flux, whereas the aphotic zone $^3$He–$NO_3$ anomaly pattern potentially has a longer persistence.

The $^3$He–$NO_3$ relationship appears much more complex within the cyclonic eddy C1 (Fig. 6B). Here there is substantial scatter toward much higher $^3$He over a range of nitrate values. The spread of $\delta^3$He points along the bottom axis corresponds to the euphotic zone samples where nitrate has been stripped and the $^3$He remains. However, the large cloud of points that populate the graph to the right of the regional flux line indicate that there either has been incomplete removal of nitrate in the absence of gas exchange, or substantial mixing between the euphotic zone nitrate-free, $^3$He-rich and aphotic zone waters that fall on the regional flux line. The former situation would imply some form of micro-nutrient limitation, or vertical convection that occurs more rapidly than nutrient uptake timescales. The latter case would require mixing of previously upwelled euphotic zone waters back down into the aphotic zone, where many of these anomalous points lie. Alternatively, if the water mass inside the eddy is of remote origin (McGillicuddy et al., 2007) it is possible that regional flux line used here may not be appropriate. Examination of data from the CLIVAR lines A20 and A22 reveals a 15% lower slope to the regional flux line. Such a decrease could work toward bringing some of the points into qualitative agreement with the conceptual model illustrated in Fig. 5, but not completely.

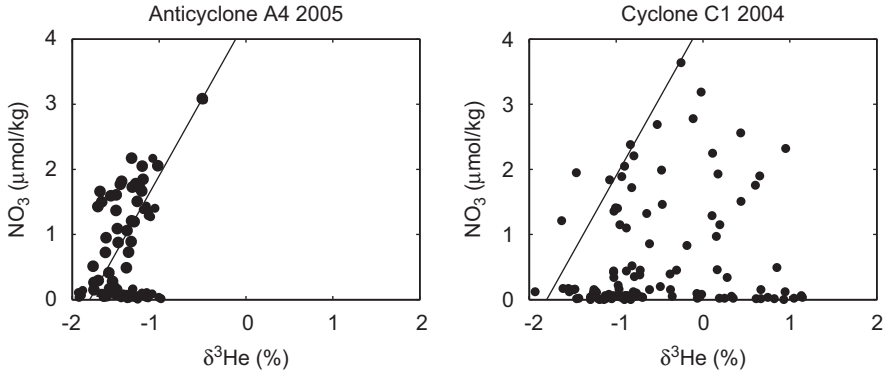


**Fig. 6.** The observed $^3$He–$NO_3$ relationship for anticyclone A4 (left panel) and cyclone C1 (right panel) in the upper 200 m.

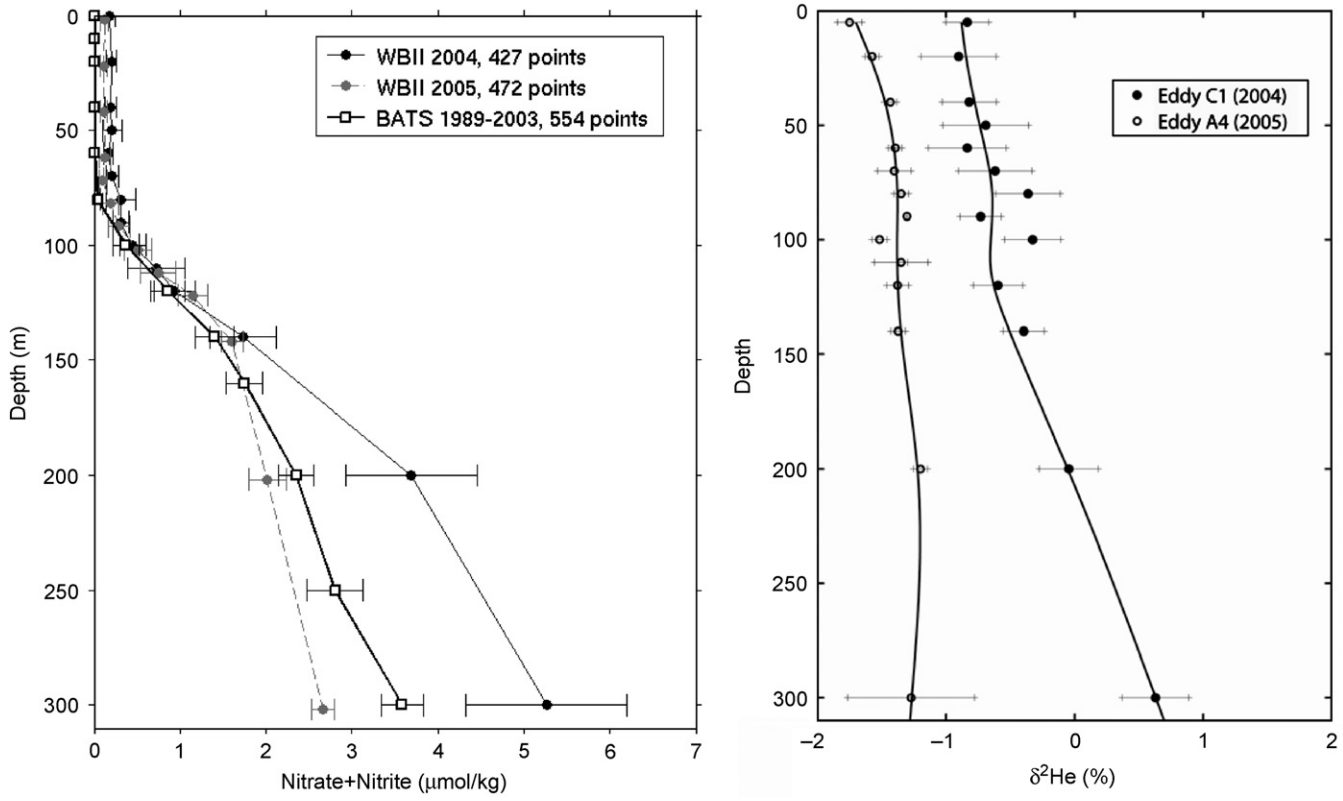


**Fig. 7.** Average depth profiles of nitrate (left panel) and $\delta^3$He for cyclonic eddy C1 (gray filled circles) and anticyclonic eddy A4 (black, filled circles). Included also for reference is the summer mean nitrate profile (open squares) for the BATS station. The error bars are standard errors of the distributions, and are larger in the $\delta^3$He case due to a smaller number of measurements.

Eddy-averaged profiles of nitrate and $\delta^3$He from C1 and A4 (Fig. 7) further illuminate differences between the two eddies. The cyclone shows anomalously higher nitrate values, with greater variability below 150 m in the aphotic zone, both compared to the anticyclone and the "background" average BATS profiles. It is noteworthy that although the profiles appear to converge toward the surface, C1 shows systematically elevated nitrate levels within the euphotic zone, compared to both BATS and A4. This excess is more strongly reflected in the $\delta^3$He profiles where there is a substantial, systematic $\delta^3$He excess throughout the euphotic zone. Interestingly, the apparent aphotic zone nitrate and $\delta^3$He surplus at 300 m depth matches the regional $NO_3$:$\delta^3$He ratio of 2.4 μmol kg$^{-1}$ %$^{-1}$, suggesting that the supply of excess nutrients to the eddy at this depth is mediated by physical processes (lateral mixing and advection). Nonetheless, that the ratio declines toward the euphotic zone, implies that vertical exchange may play a role in the nutrient and $\delta^3$He balance above 300 m.

## 5. Conclusions

Although $^3$He tracer measurements have been used extensively for inference about large-scale ocean circulation and biological processes (Jenkins, 1988b, 1998), to our knowledge this is the first attempt to apply this methodology to mesoscale phenomena.

The striking aspect of the observations, supported by the detailed profiling results of the Video Plankton Recorder (McGillicuddy et al., 2007) is that there are substantial variations and hence property gradients on scales shorter than our station spacing. There are sharp spatial changes in the $^3$He and nitrate relationships over small distances, particularly for the cyclonic eddy. The implication is that biological and physical processes are robustly occurring on those scales, and that in the absence of spatially resolving these "events" we must rely on property–property relationships and crude inventories to constrain their nature and impact.

The observations presented herein reveal clear eddy-driven imprints on $^3$He distributions, and striking differences in $^3$He–$NO_3$ relationships between the two eddy features we studied. Anticyclone A4 shows the expected idealized behavior of steady upwelling, qualitatively consistent with the mechanism of eddy–wind interactions presented in McGillicuddy et al. (2007) and Ledwell et al. (2008). In contrast, cyclone C1 shows evidence of recent significant upwelling with incomplete nitrate uptake. The detailed $^3$He–$NO_3$ relationship and its spatial distribution in cyclone C1 is suggestive of significant exchange between aphotic and euphotic zone waters. The relict flux estimate of 1.4 molN m$^{-2}$ is approximately 2–3 times annual new production for the region (Jenkins and Goldman, 1985; Jenkins, 1988a, b). Thus, such episodic processes could potentially have a significant impact on basin-scale biogeochemical budgets.

## References

Anderson, L.A., Sarmiento, J.L., 1994. Redfield ratios of remineralization determined by nutrient data-analysis. Global Biogeochemical Cycles 8 (1), 65–80.

Benson, B.B., Krause Jr., D., 1980. Isotopic fractionation of helium during solution: a probe for the liquid state. Journal of Solution Chemistry 9, 895–909.

Buesseler, K.O., Lamborg, C., Cai, P., Escoube, R., Johnson, R., Pike, S., Masque, P., McGillicuddy, D., Verdeny, E., 2008. Particle fluxes associated with mesoscale eddies in the Sargasso Sea. Deep-Sea Research II, this issue [doi:10.1016/j.dsr2.2008.02.007].

Clarke, W.B., Jenkins, W.J., Top, Z., 1976. Determination of tritium by spectrometric measurement of $^3$He. International Journal of Applied Radiation and Isotopes 27, 515–525.

Eppley, R.W., Peterson, B.J., 1979. Particulate organic matter flux and planktonic new production in the deep ocean. Nature 282, 677–680.
Holand, P.W., Emerson, D.E., 1987. A determination of the He-4 content of near-surface atmospheric air within the continental United States. Journal of Geophysical Research 92 (B12), 12557–12566.
Jenkins, W.J., 1977. Tritium–helium dating in the Sargasso Sea: a measurement of oxygen utilization rates. Science 196 (4287), 291–292.
Jenkins, W.J., 1980. Tritium and $^3$He in the Sargasso Sea. Journal of Marine Research 38, 533–569.
Jenkins, W.J., 1984. The use of tracers and water masses to estimate rates of respiration. In: Hobbie, J.E., Williams, P.L. (Eds.), Heterotrophic Activity in the Sea. Plenum Press, New York, pp. 391–403.
Jenkins, W.J., 1988a. Nitrate flux into the euphotic zone near Bermuda. Nature 331, 521–523.
Jenkins, W.J., 1988b. Using anthropogenic tritium and $^3$He to study subtropical gyre ventilation and circulation. Philosophical Transactions of the Royal Society (London) A 325, 43–61.
Jenkins, W.J., 1998. Studying thermocline ventilation and circulation using tritium and $^3$He. Journal of Geophysical Research 103 (C8), 15817–15831.
Jenkins, W.J., Doney, S.C., 2003. The subtropical nutrient spiral. Global Biogeochemical Cycles 17 (4), 1110.
Jenkins, W.J., Goldman, J.C., 1985. Seasonal oxygen cycling and primary production in the Sargasso Sea. Journal of Marine Research 43, 465–491.
Jenkins, W.J., Wallace, D.W.R., 1992. Tracer-based inferences of new primary production in the sea. In: Falkowski, P.G., Woodhead, A.D. (Eds.), Primary Production and Biogeochemical Cycles in the Sea. Plenum, New York, pp. 299–316.
Ledwell, J.R., McGillicuddy, Jr., D.J., Anderson, L.A., 2008. Nutrient flux into an intense deep chlorophyll layer in a mode water eddy. Deep-Sea Research II, this issue [doi:10.1016/j.dsr2.2008.02.005].
Lewis, M.R., Harrison, W.G., Oakey, N.S., Hebert, D., Platt, T., 1986. Vertical nitrate fluxes in the oligotrophic ocean. Science 234, 870–873.
Lott, D.E., Jenkins, W.J., 1984. An automated cryogenic charcoal trap system for helium isotope mass spectrometry. Review of Scientific Instruments 55 (12), 1982–1988.
Lott, D.E., Jenkins, W.J., 1998. Advances in the analysis and shipboard processing of tritium and helium samples. International WOCE Newsletter 30, 27–30.
Lucas, L.L., Unterweger, M.P., 2000. Comprehensive review and critical evaluation of the half-life of tritium. Journal of Research of the National Institute of Standards and Technology 105 (4), 541–549.
Martin, A.P., Richards, K.J., 2001. Mechanisms for vertical nutrient transport within a North Atlantic mesoscale eddy. Deep-Sea Research II 48 (4–5), 757–773.
McGillicuddy Jr., D.J., Robinson, A.R., 1997. Eddy-induced nutrient supply and new production in the Sargasso Sea. Deep-Sea Research I 44, 1427–1450.
McGillicuddy Jr., D.J., Robinson, A.R., Seigel, D.A., Jannasch, H.W., Johnson, D., Dickey, T.D., McNeil, J., Michaels, A.F., Knap, A.H., 1998. Influence of mesoscale eddies on new production in the Sargasso Sea. Nature 394 (6688), 263–268.
McGillicuddy Jr., D.J., Anderson, L.A., Doney, S.C., Maltrud, M.E., 2003. Eddy-driven sources and sinks of nutrients in the upper ocean: results from a 0.1° resolution model of the North Atlantic. Global Biogeochemical Cycles 17 (2).
McGillicuddy, D.J., Anderson, L.A., Bates, N.R., Bibby, T., Buesseler, K., Carlson, C., Davis, C.S., Ewart, C., Falkowski, P.G., Goldthwait, S.A., Hansel, D.A., Jenkins, W.J., Johnson, R., Kosnyrev, V.K., Ledwell, J.R., Li, Q.P., Siegel, D.A., Steinberg, D.K., 2007. Eddy–wind interactions stimulate extraordinary mid-ocean plankton blooms. Science 316, 1021–1026.
Musgrave, D.L., Chou, J., Jenkins, W.J., 1988. Application of a model of upper-ocean physics for studying seasonal cycles of oxygen. Journal of Geophysical Research 93, 15679–15700.
Oliver, B.M., Bradley, J.G., Farrar, H.I., 1984. Helium concentration of the earth's lower atmosphere. Geochimica et Cosmochimica Acta 48, 1759–1767.
Oschlies, A., 2001. Model-derived estimates of new production: new results point towards lower values. Deep-Sea Research II 48, 2173–2197.
Oschlies, A., 2002. Can eddies make ocean deserts bloom? Global Biogeochemical Cycles 16 (4), 1106.
Pelegri, J.L., Csanady, G.T., 1991. Nutrient transport and mixing in the Gulf Stream. Journal of Geophysical Research 96 (C2), 2577–2583.
Pelegri, J.L., Csanady, G.T., Martins, A., 1996. The North Atlantic nutrient stream. Journal of Oceanography 52, 275–299.
Spitzer, W.S., Jenkins, W.J., 1989. Rates of vertical mixing, gas exchange and new production: estimates from seasonal gas cycles in the upper ocean near Bermuda. Journal of Marine Research 47, 169–196.
Wanninkhof, R., 1992. Relationship between wind speed and gas exchange over the ocean. Journal of Geophysical Research 97 (C5), 7373–7382.
Williams, R.G., Follows, M.J., 1998. The Ekman transfer of nutrients and maintenance of new production over the North Atlantic. Deep-Sea Research I 45 (2–3), 461–489.
Williams, R.G., Roussenov, V.M., Follows, M.J., 2006. Nutrient streams and their induction into the mixed layer. Global Biogeochemical Cycles 20 (GB1016), (2005GB002586).